scientific reports

Check for updates

OPEN

Hypoxia-induced TPC2 transcription and glycosylation aggravates pulmonary arterial hypertension by blocking autophagy flux

Chao Li[1], Cheng Li[1], YuFei Jiang[1,2], MoFei Liu[1], ChengYi Yang[1], JiaXin Lu[1] & YongLiang Jiang[1]✉

Pulmonary arterial hypertension (PAH) is a serious medical condition that causes a failure in the right heart. Two-pore channel 2 (TPC2) is upregulated in PAH, but its roles in PAH remain largely unknown. Our investigation aims at the mechanisms by which TPC2 regulates PAH development. We established an experimental PAH rat model via monocrotaline administration. Human and rat pulmonary arterial smooth muscle cells (PASMCs) were treated hypoxia as in vitro cell PAH models. The thickness of pulmonary arterial wall and obstructive arteriopathy in rats were examined. Autophagy was detected through TEM, and Ca^{2+} measurement and mRFP-GFP-LC3 transfection. The expression of α-SMA, LC3, p62, TPC2, HIF1α and STT3B were analyzed by qRT-PCR, western blot or IHC staining. The binding of HIF1α to TPC2 promoter was determined by ChIP-qPCR and EMSA assays. TPC2 glycosylation was evaluated by western blot. Transwell assay was applied to analyze cell migration. TPC2 expression was promoted and autophagy was inhibited in PAH rats and hypoxia-treated PASMCs. HIF1α directly bound to the promoter of TPC2, thus transcriptionally activating its expression in PAH rats and hypoxic PASMCs. Knockdown of TPC2 facilitated autophagic flux and repressed PASMC migration. STT3B enhanced TPC2 glycosylation in hypoxic PASMCs. Furthermore, Overexpression of TPC2 suppressed autophagic flux and promoted PASMC migration, but these effects were abrogated by STT3B knockdown or PNGase F, an eraser of N-linked glycans. Suppression of TPC2 enhanced autophagy and alleviated PAH in vivo. HIF1α-induced TPC2 transcription and subsequent STT3B-dependent TPC2 glycosylation inhibit autophagic flux and aggravate PAH. Our study suggests TCP2 as a potential therapeutic target for PAH.

Keywords Pulmonary arterial hypertension, Autophagy, Glycosylation, HIF1α, TPC2, STT3B

Pulmonary arterial hypertension (PAH) is a devastating disease characterized by high blood pressure that affects pulmonary artery and heart[1]. Damage to the lining of pulmonary artery may cause PAH. Although not causal, the dysfunction and hypoxia of endothelial cells generally aggravate PAH[2]. The symptoms of PAH include weakness, chest pain, breathlessness and fatigue, and PAH eventually causes right heart failure and death[3]. Unfortunately, there is still no cure for PAH although great progress has been made in PAH therapies recently. PAH treatments are generally divided into general supportive therapies such as limiting fluid, salt intake and supplemental oxygen, and PAH specific therapies including phosphodiesterase-5 (PDE5) inhibitors, calcium channel blockers, drugs targeting endothelin and prostacyclin pathways[2,4]. If therapies do not work, lung transplantation may be the last opportunity for patients. Thus, exploring the mechanisms underlying the pathogenesis of PAH is essential for developing novel targeted therapies for PAH.

Two-pore channels (TPCs) are voltage-gated cation channels that are found in endosome and lysosome membranes and play key roles in regulating intracellular Ca^{2+}. TPCs are divided into TPC1, 2 and 3, and only TPC1 and 2 are found in mouse and human cells. TPC2 is predominantly expressed in late endosome and

[1]Department of Respiratory Medicine, Hunan Provincial People's Hospital (The First-Affiliated Hospital of Hunan Normal University), No. 61 Jiefang Xi Road, Changsha, Hunan 410219, China. [2]Faculty of Healthy Science, University of Macau, Macau 999078, China. ✉email: yvfei316@163.com

lysosome[5]. TPC2 is more selective for Ca^{2+} and contributes to releasing more Ca^{2+} than TPC1[6]. Hu and colleagues observed that loss of TPC2 inhibited acetoxymethyl ester derivative of nicotinic acid adenine dinucleotide phosphate (NAADP-AM)-induced calcium flux and extracellular matrix in endothelial cells, but silencing of TPC1 hardly caused any physiological changes[7]. Both TPC1 and 2 are found in rat pulmonary arterial smooth muscle cells (PASMCs), and hypoxia can induce their expression[8,9]. TPC2 increases autophagosomes with elevated lysosomal pH in cancer cells by repressing the fusion of autophagosome and lysosome[10]. Autophagy is associated with PAH although the evidence is very limited[11,12]. In this study, we hypothesized that TPC2 might inhibit autophagy via regulating lysosomal Ca^{2+} in PASMCs, contributing to PAH progression.

N-linked glycosylation, a key post-translational modification, refers to coupling glycans or oligosaccharides to the asparagine residues of proteins that modulates protein folding, targeting, stability and function[13]. N-glycosylation widely affects ion channels on the plasma membrane[14,15], but its involvement in the modulation of intracellular ion channels is largely unknown. TPC 2 is N-glycosylated at residues 599 and 611[16]. A previous study has suggested that hypoxia induces the N-glycosylation of CD133 to repress its degradation and alter biological activity in glioma[17]. However, the mechanisms underlying TPC2 glycosylation and its role in the regulation of PAH progression are unknown. Oligosaccharyltransferase Complex Catalytic Subunit B (STT3B) initiates N-glycosylation of target proteins[18], but the interaction between STT3B and TPC2 has not been reported.

Thus, uncovering the involvement of TPC2 and STT3B in PAH deepens the understanding of PAH pathogenesis. In this study, we found that HIF1α activated TPC2 transcription, and subsequently STT3B promoted TPC2 glycosylation, by which autophagy was suppressed in hypoxia-treated PASMCs. We demonstrated that hypoxia could induce TPC2 expression and subsequent STT3B-dependent glycosylation, thereby exacerbating PAH via suppressing autophagic flux. Our findings provide novel insights into PAH pathogenesis and suggest novel therapeutic targets for PAH.

Methods

Cell culture and transfection

Primary rat and human pulmonary artery smooth muscle cells (RPASMCs and HRASMCs) were provided by Sigma-Aldrich (St. Louis, MO, USA) and the American Type Culture Collection (ATCC, Manassas, VA, USA) respectively and maintained in DMEM/10% FBS (Thermo Fisher Scientific, Waltham, MA, USA) culture medium in a cell incubator. For hypoxia treatment, PASMCs were cultured in a hypoxic condition (5% O_2) for 24 h, and cells in the normoxia group were maintained in an incubator of 5% CO_2. To inhibit glycosylation, PASMCs were treated with PNGase F (New England Biolabs, Ipswich, MA, USA) at 25 U/mL for 12 h. Coding sequences for HIF1α (OE-HIF1α) and TPC2 (OE-TPC2) were cloned into pcDNA3.1 (Thermo Fisher Scientific). ShRNA constructs for HIF1α (sh-HIF1α), TPC2 (sh-TPC2), STT3A (sh-STT3A) and STT3B (sh-STT3B) and scramble negative controls (sh-NC) were provided by RiboBio (Guangzhou, China). PASMCs were transfected with overexpressing or shRNA knockdown constructs with Lipofectamine 3000 (Thermo Fisher Scientific) following the manual. After 60 h, cells were collected for subsequent analysis.

Rat model of PAH

Rat model of PAH was established as previously described[19]. For PAH modeling, Sprague–Dawley rats (male, 200–250 g) provided by from Human SJA Laboratory Animal Co., Ltd. (Changsha, China) were subcutaneously injected with monocrotaline (Sigma-Aldrich) at 60 mg/kg in the ventral thorax and maintained for 4 weeks. Rats received administration of rapamycin (2 mg/kg, Sigma-Aldrich), chloroquine (1 mg/kg, Sigma-Aldrich), PNGase F (100 U/kg) or Ned-19 (2 mg/kg, Sigma-Aldrich) every three days through gavage. Animal experiments were approved by the Ethics Committee of Hunan Provincial People's Hospital.

For hypoxia-induced PAH modeling, Sprague–Dawley rats (male, 200–250 g) provided by from Human SJA Laboratory Animal Co., Ltd. (Changsha, China) were exposed to 10% inspired O2 (Partial Pressure of Oxygen 40 mm Hg) for 4 weeks to establish a rat model of chronic hypoxia-induced PAH.

Transmission electron microscopy (TEM)

Autophagy in PASMCs was monitored via TEM as previously described[20]. Briefly, PASMCs were fixed in 2% glutaraldehyde, scraped and pelleted followed by wash in HEPES and PBS. Then, pellets were incubated in 1% osmium tetroxide for 1 h and stained in 2% uranyl acetate prior to dehydration in 70%, 95% and 100% ethanol and propylene oxide. Pellets were incubated in 1:1 resin/propylene oxide for 2 h and subsequently in resin overnight. Pellets were transferred in fresh resin, and the blocks were polymerized. Sections (80 nm) were prepared, picked up on 200 mesh grids for staining in with 2% uranyl acetate and 0.3% lead citrate and imaged using a TEM (Thermo Fisher Scientific).

Ca^{2+} measurement

For measuring lysosomal Ca^{2+}, PASMCs were incubated with Fluo4/AM (150 μg/mL, Thermo Fisher Scientific) overnight at 37 ℃. After wash, the fluorescence was recorded at Ex/Em = 494/506 nm.

Autophagic flux analysis

mRFP-GFP-LC3 adenovirus from Hanbio (Shanghai, China) was used to detect autophagic flux in PASMCs. PASMCs were infected with mRFP-GFP-LC3 (5×10^9 PFU/mL), and cells were fixed in 4% formaldehyde. After wash, green and red fluorescence were detected under a confocal microscope (Nikon, Tokyo, Japan).

Hematoxylin and eosin stain (H&E) and immunohistochemistry (IHC) staining

Pulmonary arteries were fixed, dehydrated and embedded in paraffin. Subsequently, 5 μm of sections were prepared and dewaxed in xylene. After rehydration, sections were stained with hematoxylin for 5 min, washed

5 times in water and processed to stained in eosin for 30 s. Then, sections were dehydrated, cleared in xylene and mounted. For IHC staining, paraffin sections were processed to antigen retrieval in pH 6.0 citrate buffer (Abcam, Cambridge, UK). After block, sections were incubated with an anti-α-SMA (Proteintech, 14395–1-AP, 1:1000), anti-LC3 (Proteintech, 14600–1-AP, 1:300), anti-p62 (Abcam, ab109012, 1:200) or anti-TPC2 (Abcam, ab119915, 1:100) overnight. Sections were washed and incubated with a goat anti-rabbit HRP antibody (Servicebio, GB23303, 1:2000), and DAB (Beyotime, Shanghai, China) was added for signal visualization followed by hematoxylin staining. Sections were mounted and imaged. All antibodies used in IHC were obtained from Abcam.

Chromatin immunoprecipitation quantitative PCR (ChIP-qPCR)

PASMCs ($\sim 1 \times 10^7$) were crosslinked in 2% formaldehyde for 20 min and rinsed, and cell lysis buffer supplemented with protease inhibitors (Thermo Fisher Scientific) was added. After 15 min, cell lysates were collected and processed to ultrasonication for generating DNA fragments with a length of ~ 500 bp. Then, cell lysates were centrifugated for 20 min, and supernatants were collected. An anti-HIF1α (5 μg, CST, #14179), anti-Pol II (5 μg, Abcam, ab193468) or anti-H3K27ac (5 μg, Abcam, ab4729) was mixed with the supernatants and incubated overnight at 4 ℃. Subsequently, magnetic protein A/G beads (Merck Millipore, Burlington, MA, USA) was added and incubated for additional 2 h. Samples were placed in magnet for wash, and DNA was recovered. The enrichment of TPC2 promoter was analyzed by quantitative PCR.

Electrophoretic mobility shift assays (EMSA)

Nuclear protein extracts from PASMCs were prepared with NE-PER Extraction Reagent (Thermo Fisher Scientific) and subjected to EMSA. Unlabeled and biotin-labeled TPC2 promoter were synthesized by Sangon (Shanghai, China). EMSA assays were performed using LightShift Chemiluminescent EMSA Kit from Thermo Fisher Scientific according to the manufacturer's recommendations, and addition of an anit-HIF1α (2 μg, CST, #14179) caused supershift in electrophoresis.

Transwell assay

The 8 μm transwell chamber (Corning, Corning, NY, USA) was used for analyzing PASMC migration. PASMCs were seeded into the upper chamber, and the lower chamber was filled with fresh medium. Subsequently, cells were cultured for 24 h for penetration of cells into the lower surface. Then, migratory cells to the lower surface were fixed and stained with crystal violet (Sigma-Aldrich) for 15 min. After wash, cells were air dried and imaged.

Real-time quantitative reverse transcription PCR (qRT-PCR)

RNA was isolated from PASMCs and rat pulmonary arteries using E.Z.N.A.® Total RNA Kit I (Omega Biotek, Norcross, GA, USA) following the manual and reversely transcribed into cDNA with PrimeScript High Fidelity RT-PCR Kit (Takara, Shiga, Japan). The expression of TPC2, HIF1α, STT3A and STT3B was examined by quantitative PCR. GAPDH was used as a normalization control, and the $2^{-\Delta\Delta Ct}$ method was applied. Primers were listed in Table 1.

Western blot

Protein was extracted from PASMCs and rat pulmonary arteries using protein extraction buffer (Beyotime) supplemented with protease inhibitors and quantified with Bradford Protein Assay Kit from Beyotime. Protein (30 μg) was loaded for electrophoresis and transferred to PVDF membranes (Bio-Rad, Hercules, CA, USA). Antibodies against anti-α-SMA (Proteintech, 14395-1-AP, 1:1000), anti-LC3 (Proteintech, 14600-1-AP, 1:300), anti-p62 (Abcam, ab109012, 1:200) or anti-TPC2 (Abcam, Ab119915, 1:100) and HIF1α (CST, #14179, 1:500) were used to examine their abundance. GAPDH was used a normalization control.

Statistical analysis

Results were from three independent experiments and showed as mean ± standard deviation (SD). *SPSS* Statistics 17.0 was applied for statistical analysis. Fisher's least significant difference (LSD) method was used for comparisons of multiple groups. Significance in all figures was indicated as follows: *: $P < 0.05$, **: $P < 0.01$, ***: $P < 0.001$, N.S.: not significant.

Results

TPC2 expression was enhanced and autophagy was inhibited in PAH rats

We established an experimental PAH rat model via monocrotaline administration to explore the implication of TPC2 and autophagy in PAH. Compared to rats in the control group, monocrotaline-treated rats showed increased haematocrit (HCT), heart rate, heart hypertrophy (measured as RV/(LV + S)) (Table 2) and thickness of pulmonary arterial wall and obstructive arteriopathy (Fig. 1A). Moreover, elevated abundance of α-SMA in pulmonary arterial tissues from monocrotaline-treated rats was observed (Fig. 1B and C). These observations confirmed that PAH was successfully modeled in rats. As N-glycosylated TPC2 is an important regulator of autophagic flux[21,22], we further examined the expression of two autophagy markers LC3 and p62 and quantified the ratio of LC3 II to LC3 I. Decreased ratio of LC3 II to LC3 I suggested that the conversion of LC3 I to LC3 II was inhibited, but p62 was upregulated in PAH rats (Fig. 1D and E), suggesting that autophagy might be suppressed in PAH. Besides, we found that TPC2 was upregulated in pulmonary arterial tissues from PAH rats (Fig. 1F–H). Collectively, these observations in PAH rats showed that the expression of TPC2 was promoted and autophagy was suppressed in PAH. Furthermore, PAH rats were administrated with the autophagy inhibitor bafilomycin A1 (Baf A1). The thickened pulmonary arterial wall and obstructive arteriopathy, increased α-SMA and p62 expression, and downregulation of LC3 in the pulmonary aorta and lung were not changed in PAH rats

Rat *Tpc2*	**Forward: 5′-TCACCGTAATCGGGATGCTG-3′**
	Reverse: 5′-CAAGCTTCCATCAGGGTTGT-3′
Rat *Hif1α*	Forward: 5′-CAACCTCACCAGACAGAGCA-3′
	Reverse: 5′-TGCTGCAGTAACGTTCCAATTC-3′
Rat *Stt3a*	Forward: 5′-GCTCCTCATCCTGTCGATGG-3′
	Reverse: 5′-GTACCAAGCCCGGTCATCAA-3′
Rat *Stt3b*	Forward: 5′-CTCATGGCTCTGGGGAACAG-3′
	Reverse: 5′-GATGATGCTCTCGAAGCGGA-3′
Rat *Gapdh*	Forward: 5′-GCAAGTTCAACGGCACAG-3′
	Reverse: 5′-GCCAGTAGACTCCACGACAT-3′
Human *Tpc2*	Forward: 5′-TGCATTGATCAGGCTGTGGT-3′
	Reverse: 5′-GAAGCTCAAAGTCCGTTGGC-3′
Human *Hif1α*	Forward: 5′-AGAGGTTGAGGGACGGAGAT-3′
	Reverse: 5′-GACGTTCAGAACTTATCCTACCAT-3′
Human *Stt3a*	Forward: 5′-GAACGGATGGCTGAGGGAG-3′
	Reverse: 5′-ACACACGACGATCAGTTTGC-3′
Human *Stt3b*	Forward: 5′-CGAGTTCGACCCGTGGTTTA-3′
	Reverse: 5′-GCCGCTAAAAGTTGGTGCAA-3′
Human *Gapdh*	Forward: 5′-CTGACTTCAACAGCGACACC-3′
	Reverse: 5′-GTGGTCCAGGGGTCTTACTC-3′

Table 1. qRT-PCR primers.

Group	RV/(LV + S)	HCT (%)	mPAP (mmHg)	mAP (mmHg)	HR
PAH (n = 5)	0.53 ± 0.03	59.7 ± 1.31	39.75 ± 1.03	98.7 ± 5.4	384.2 ± 3.5
PAH + Rapa (n = 5)	0.31 ± 0.02	38.9 ± 0.98	24.83 ± 0.86	90.7 ± 4.9	396.5 ± 3.7
PAH + CQ (n = 5)	0.49 ± 0.04	58.7 ± 1.22	37.29 ± 1.12	97.9 ± 6.3	383.7 ± 2.9
PAH + PNGase F (n = 5)	0.35 ± 0.03	42.6 ± 1.08	25.86 ± 0.93	91.4 ± 5.2	395.3 ± 3.8
PAH + ned-19 (n = 5)	0.34 ± 0.02	40.1 ± 1.06	26.27 ± 1.11	92.3 ± 4.7	393.6 ± 3.2

Table 2. Data analysis of different processing groups.

treated with Baf A1 (Fig. 1A–F). Moreover, increased expression of TPC2 in PAH rats was also not affected by Baf A1 treatment (Fig. 1G and H). These data suggested that Baf A1 treatment did not affect autophagy in PAH rats.

TPC2 expression and autophagic flux were dysregulated in hypoxia-treated PASMCs

As hypoxia is highly associated with pulmonary hypertension[23], we treated human and rat pulmonary arterial smooth muscle cells (HPASMCs and RPASMCs) with an hypoxic condition to evaluate the changes of TPC2 and autophagy in hypoxia-related PAH. Hypoxia treatment greatly enhanced cell migration and proliferation compared to normoxia treatment (Fig. 2A and B). Similar with PAH rats, hypoxic PASMCs showed decreased LC3 expression and ratio of LC3II/LC3I and increased p62 expression (Fig. 2C). Moreover, TEM examination showed an decreased number of autophagosomes in hypoxia-treated cells (Fig. 2D). Subsequently, mRFP-GFP-LC3 was transfected into PASMCs to assess autophagic flux. Results showed that compared to normoxic cells, hypoxic cells exhibited decreased autolysosomes ($mRFP^+$ GFP^-), indicating that hypoxia might block autophagic flux (Fig. 2E). As lysosomal Ca^{2+} were closely related to autophagy[24,25], we measured and found that lysosomal Ca^{2+} was decreased in PASMCs in response to hypoxia (Fig. 2F). Further, the expression of TPC2 was elevated in hypoxia-treated PASMCs (Fig. 2G and H). Thus, our results showed dysregulated TPC2 expression and autophagic flux in hypoxia-treated PASMCs. In addition, HPASMCs and RPASMCs were divided into normoxia, hypoxic and hypoxic + Baf A1 groups. Increased cell migration and proliferation, reduced autophagy, blocked autophagic flux, decreased lysosomal Ca^{2+} and TPC2 expression in hypoxic PASMCs were not affected by Baf A1 treatment (Fig. 2A–H), suggesting that Baf A1 did not affect autophagy in hypoxic PASMCs.

HIF1α transcriptionally activated TPC2 expression in PAH

HIF1α is a key transcription factor that controls hypoxic adaptation[26]. We examined HIF1α expression and found that HIF1α was significantly upregulated in pulmonary arterial tissues from PAH rats and hypoxic PASMCs (Fig. 3A–C). Furthermore, we found that the enrichment of the promoter of TPC2 by antibodies against HIF1α, Pol II and H3K27ac was greatly enhanced in pulmonary arterial tissues from PAH rats (Fig. 3D), suggesting that HIF1α potentially regulated TPC2 transcription. Then, we identified potential binding sites (5'-TTTCTCCCT CTTTCCC-3') for HIF1α in the promoter of TPC2 through AnimalTFDB v4.0 (https://guolab.wchscu.cn/Ani

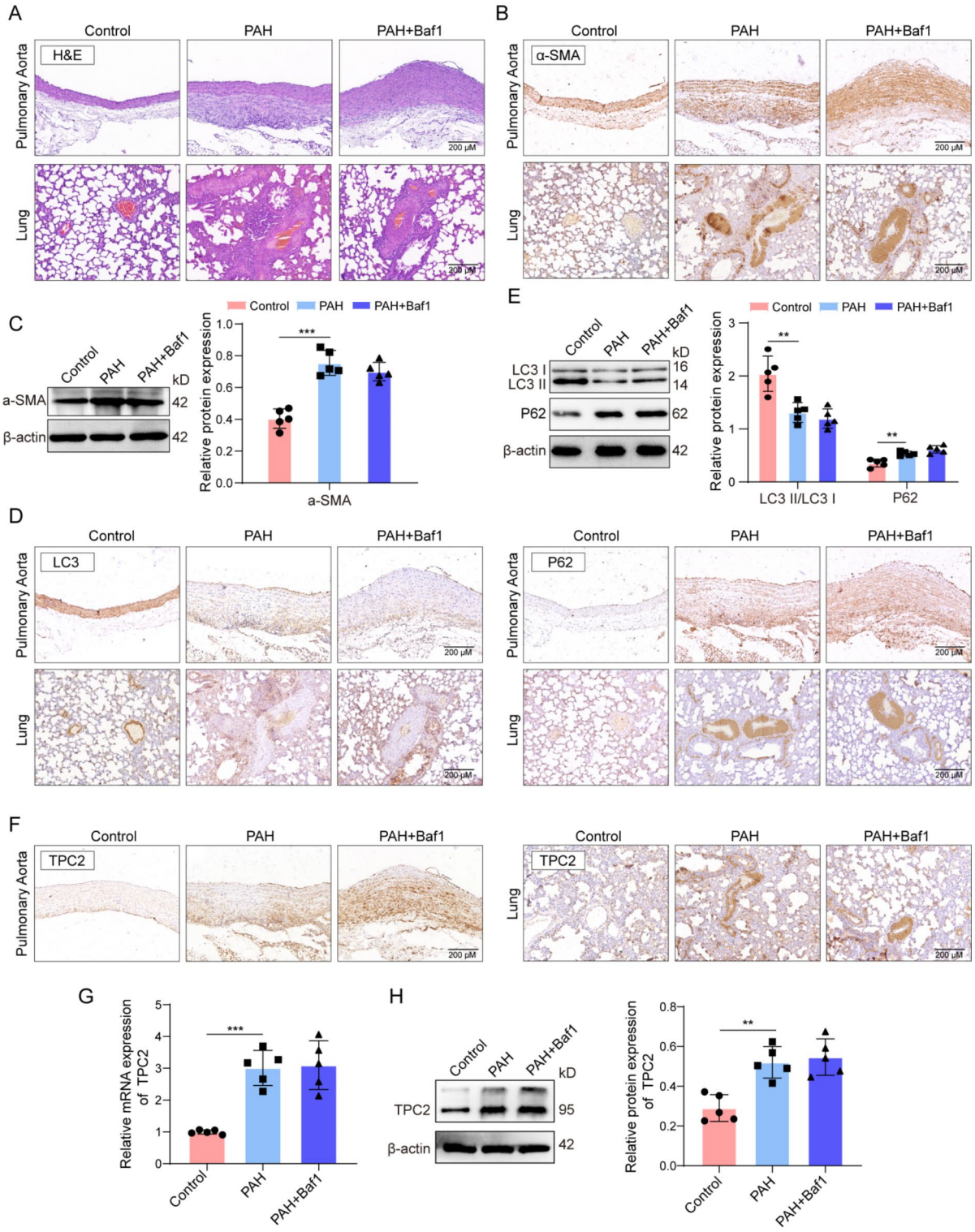

Fig. 1. TPC2 expression and autophagy were dysregulated in PAH rats. SD rats were divided into control, PAH (monocrotaline) and PAH + BafA1 groups. (n = 5) (**A**) H&E staining of pulmonary aorta and the lung. (**B**–**E**) The expression of α-SMA and LC3 was detected via IHC staining and western blot. (F–H) TPC2 was detected via IHC staining, qRT-PCR and western blot. **P < 0.01 and ***P < 0.001. Original blots/gels are presented in Supplementary Fig. 1–3.

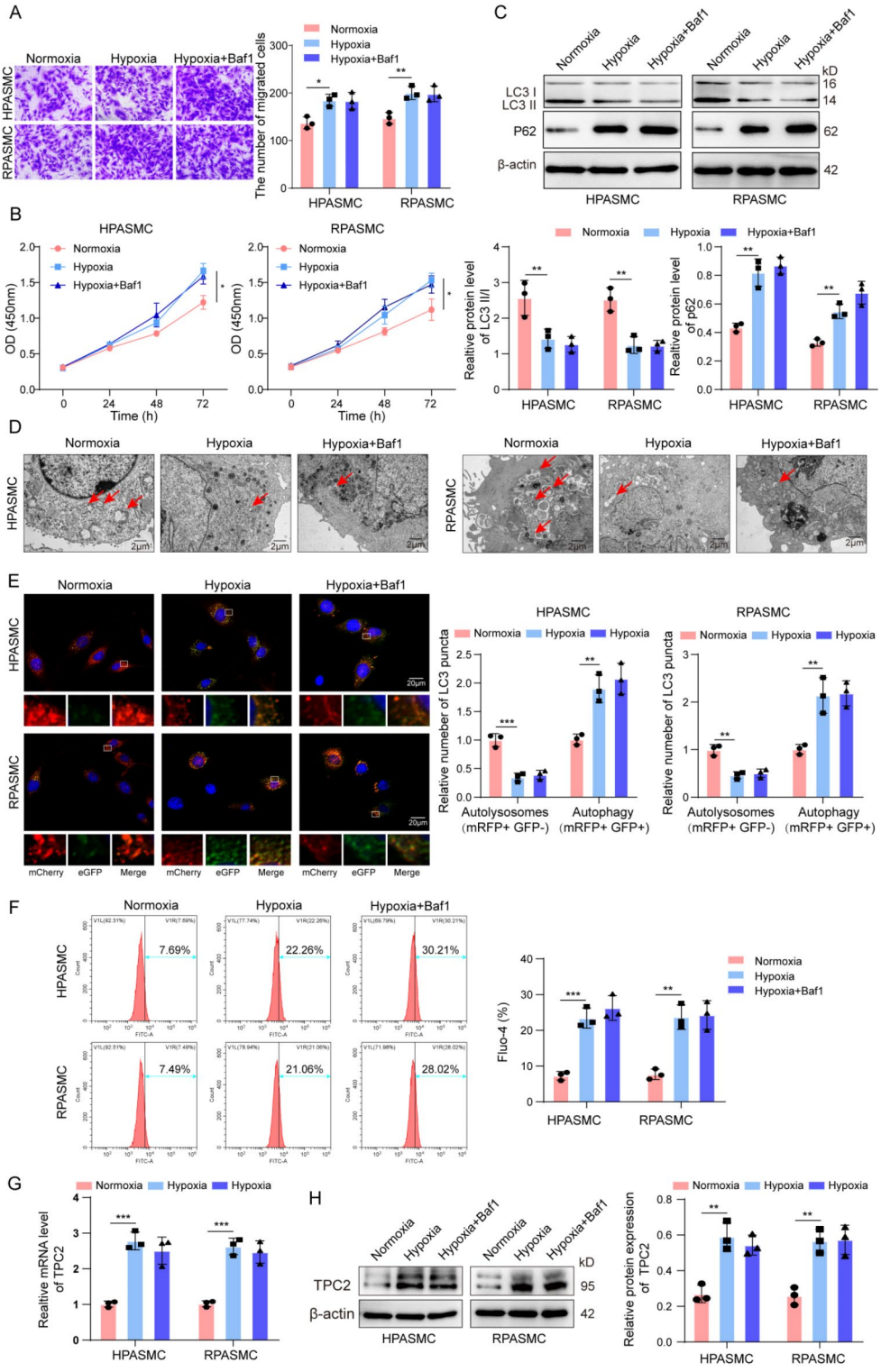

Fig. 2. The expression of TPC2 was enhanced and autophagic flux was blocked in hypoxic PASMCs. HPASMCs and RPASMCs were divided into normoxia, hypoxic and hypoxic + BafA1 groups. (**A** and **B**) Cell migration and proliferation analysis (n = 3). (**C**) The expression of LC3 and p62 was detected through western blot. (D) TEM examination of autophagy. Scale bar, 1 μm. (**E**) Autophagic flux was analyzed via mRFP-GFP-LC3 transfection. Red indicates mRFP, and Green indicates GFP. Scale bar, 20 μm. (**F**) Measurement of lysosomal Ca^{2+}. (G and H) qRT-PCR and western blot analysis of TPC2 expression (n = 3).*P < 0.05, **P < 0.01 and ***P < 0.001. Original blots/gels are presented in Supplementary Fig. 1–3.

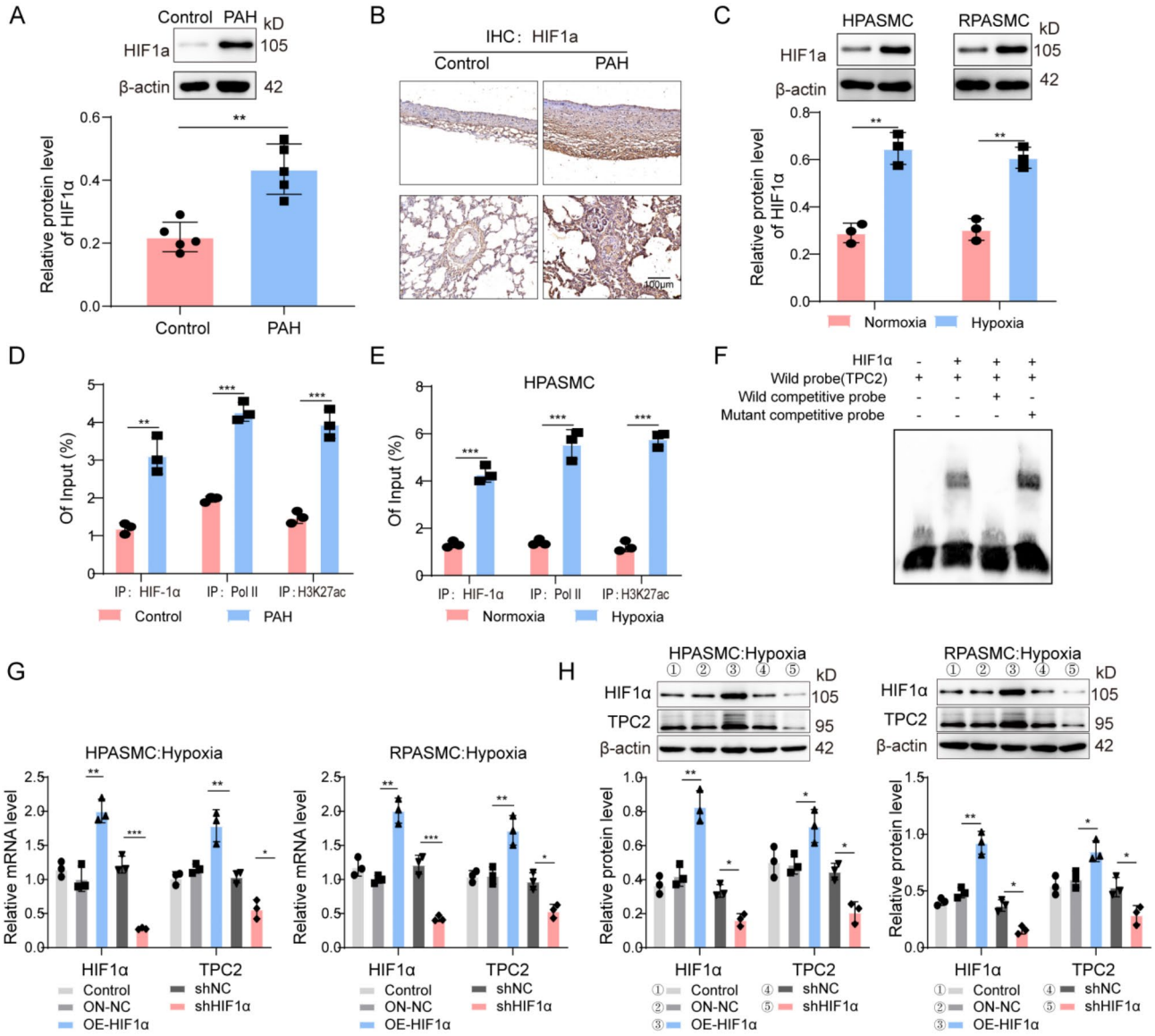

Fig. 3. HIF1α transcriptionally activated TPC2 expression in PAH. SD rats were divided into control and PAH (monocrotaline) groups, and PASMCs were treated with normoxia and hypoxia. (n = 5) (**A**–**C**) HIF1α abundance in PAH rats and PASMCs was detected through western blot and IHC. (**D** and **E**) ChIP-qPCR assays for determining the binding of HIF1α, Pol II and H3K27ac to the promoter of TPC2 in PAH rats and PASMCs. (**F**) The interaction between HIF1α and TPC2 promoter was further evaluated by EMSA assays. (**G** and **H**) qRT-PCR and western blot analysis of HIF-1α and TPC2 expression in HIF1α-overexpressing or silencing PASMCs. $^{*}P < 0.05$, $^{**}P < 0.01$ and $^{***}P < 0.001$. Original blots/gels are presented in Supplementary Fig. 1–3.

malTFDB4/#/), and increased enrichment of TPC2 promoter by antibodies against HIF1α, Pol II and H3K27ac was observed in hypoxic PASMCs compared to control cells (Fig. 3E). In addition, EMSA assays confirmed that the binding of HIF1α to TPC2 promoter was significantly enhanced in pulmonary arterial tissues from PAH rats and hypoxic PASMCs (Fig. 3F). To determine whether HIF1α regulates TPC2 expression, HIF1α was overexpressed or knocked down in PASMCs, and cells were cultured in a hypoxic condition (5% O2) for 24 h (Fig. 3G and H). We found that overexpression of HIF1α facilitated TPC2 expression, whereas knockdown of HIF1α repressed TPC2 expression in hypoxic PASMCs (Fig. 3G and H). Our findings showed that HIF1α transcriptionally activated TPC2 expression via directly binding to its promoter.

TPC2 affected lysosomal Ca^{2+} release and inhibited autophagosome-lysosome fusion in hypoxic PASMCs

We further determined TPC2-mediated regulation of autophagy in hypoxia-treated human and rat PASMCs. Results showed that silencing of TPC2 enhanced autophagy in hypoxia-treated PASMCs (Fig. 4A). Moreover, silencing of TPC2 elevated lysosomal Ca^{2+} (Fig. 4B). Additionally, autolysosomes ($mRFP^{+}$ GFP^{-}) was increased

in TPC2-silencing cells (Fig. 4C). p62 was downregulated, and LC3 expression and LC3II/LC3I ratio were upregulated in TPC2-silencing PASMCs (Fig. 4D). Furthermore, we found that knockdown of TPC2 inhibited the migration of hypoxic PASMCs (Fig. 4E). Our results suggest that inhibition of TPC2 promotes lysosomal Ca^{2+} release and restores autophagy flux, thus suppression PASMC migration.

Hypoxia induced STT3B-mediated TPC2 glycosylation

We examined whether hypoxia induced TPC2 glycosylation in human and rat PASMCs, and found that the level of glycosylation was elevated in hypoxic PASMCs, and it was largely reduced by PNGase F, an eraser of N-linked glycans (Fig. 5A and B). As STT3A and STT3B are primary catalytic subunits of the oligosaccharyl transferase (OST) complex[27], STT3A and STT3B were knocked down in PASMCs, which was confirmed by western blot assays (Fig. 5C and D). Hypoxia-induced TPC2 glycosylation was significantly suppressed by knockdown of STT3B, but it was not affected by STT3A silencing (Fig. 5E and F). The putative glycosylation site of TPC2 was highly conserved in human, nonhuman primates and other mammals and shown in red (Fig. 5G). Thus, hypoxia induced STT3B-dependent TPC2 glycosylation in PASMCs.

STT3B-dependent TPC2 glycosylation inhibited autophagic flux and enhanced migration in hypoxic PASMCs

Subsequently, we evaluated STT3B-dependent TPC2 glycosylation-mediated regulation of autophagy. TEM examination showed that TPC2 overexpression-mediated suppression of autophagy was reversed by STT3B knockdown or PNGase F treatment in hypoxic PASMCs (Fig. 6A). Moreover, silencing of STT3B and PNGase F treatment raised lysosomal Ca^{2+} in TPC2-overexpressing PASMCs (Fig. 6B). Blocked autophagic flux in TPC2-overexpressing cells was promoted by STT3B knockdown or PNGase F treatment (Fig. 6C). Besides, Cell migration rate was suppressed by silencing of STT3B or PNGase F treatment in PASMCs with overexpression of TPC2 (Fig. 6D). Collectively, TPC2 glycosylation blocked autophagic flux and inhibited PASMC migration in response to hypoxia dependent on STT3B.

Inhibition of TPC2 promoted autophagy and alleviated PAH in rats

Rats were induced with PAH and divided into five groups: PAH, PAH + Rapamycin (an autophagy inducer), PAH + Chloroquine (an autophagy inhibitor), PAH + PNGase F and PAH + Ned-19 (a TPC2 blocker). Increased HCT, heart rate, RV/(LV + S) and thickness of pulmonary arterial wall and obstructive arteriopathy in PAH rats were mitigated by rapamycin, PNGase F or Ned-19, but no significant beneficial effects were observed in the PAH + Chloroquine group (Fig. 7A and Table 3), suggesting that inducing autophagy and blocking TPC2 could ameliorated PAH. Furthermore, increased expression of α-SMA and TPC2 and decreased LC3 expression were reversed by rapamycin, PNGase F or Ned-19, but chloroquine did not affect their expression (Fig. 7B). In addition, rapamycin, PNGase F or Ned-19 enhanced autophagy and repressed TPC2 glycosylation in the lung tissue, but chloroquine did not show these effects (Fig. 7C and D). Our findings implied that induction of autophagy and suppression of TPC2 alleviated PAH *in* vivo. In addition, Baf A1 administration did not affect pathological changes, the expression of α-SMA, TPC2 and p62, the number of autophagosome and TPC2 glycosylation in Hypoxia-induced PAH rats (Fig. 8A–D).

Discussion

Autophagy is dysregulated in various diseases such as diabetes, neurodegenerative disorders and cancers[28–30]. Emerging evidence has suggested that abnormal autophagy is implicated in the pathogenesis of PAH. PAH patients show increased autophagy with elevated expression of LC3B-II[31]. Importantly, many studies have revealed that inhibition of autophagy contributes to ameliorating PAH. Long et al. found that chloroquine could alleviate monocrotaline-induced experimental PAH in rats through suppression of autophagy[32]. In addition, paclitaxel has been reported to ameliorate experimental PAH by repressing FoxO1-mediated autophagy[33]. The mammalian target of rapamycin complex 1 (mTORC1), a well-known inhibitor of autophagy[34], is activated in PAH[35], and activation of mTOR inhibits autophagy in RPASMCs[36]. In consistence with previous studies, we also found that administration of rapamycin significantly promoted autophagy and alleviated experimental PAH in rats. TPC2 has been reported to be highly expressed in hypoxia-induced pulmonary artery endothelial cells and PAH, and silencing of TPC2 shows potential of improving PAH through suppression of calcium signaling[7]. However, the mechanisms underlying the regulation of TPC2 in PAH remain largely unknown. For the first time, we demonstrate that HIF1α transcriptionally activates TPC2 expression, and subsequently increased STT3B-dependent TPC2 glycosylation promotes PASMC proliferation in response to hypoxia and exacerbates PAH via blocking autophagy (Fig. 9), providing a novel regulatory mechanism involving TPC2 in PAH and suggesting that targeting TPC2 and autophagy may be potential approaches for PAH management.

Lysosomal Ca2 + signaling plays key roles in autophagy. Medina et al. reported that lysosomal Ca^{2+} signaling modulated autophagy by controlling calcineurin and TFEB activities[24]. During autophagy, lysosomal pH slightly decreases[25], and increased lysosomal pH may lead to autophagic flux blockage[37,38]. As TPC2 coactivation can globalize lysosomal Ca^{2+} signaling and regulate lysosomal pH[39], we evaluated the effects of TPC2 on lysosomal Ca^{2+} in PAH. As expected, suppression of TPC2 led to increased lysosomal Ca^{2+} in hypoxia-induced PASMCs. Strikingly, we found that TPC2 blocked autophagic flux by promoting lysosomal Ca^{2+} release in PASMCs exposed to hypoxia. Moreover, in experimental PAH rats, autophagy was downregulated, and rapamycin alleviated the increase of arterial wall thickness and obstructive arteriopathy, suggesting that activation of autophagy restrained the development of PAH. However, in contrast with our observation, numerous studies have shown that autophagy is promoted in hypoxic PASMCs and experimental PAH animals although autophagy exerts a protective activity[32,40,41]. We speculate that the level of autophagy may be different in various stages of PAH and increased autophagy contributes to alleviating PAH, but the microenvironment, such as increased abundance

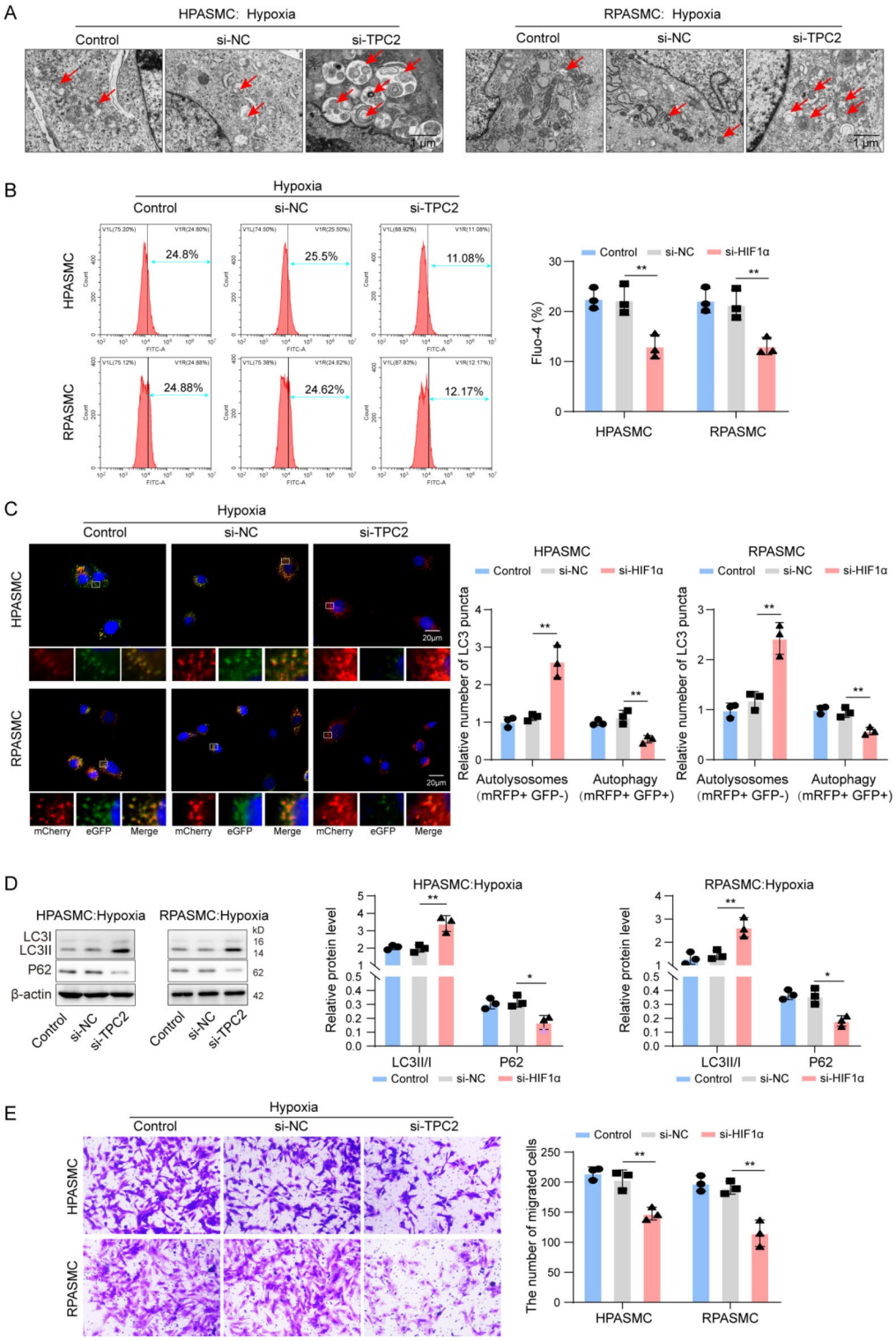

Fig. 4. The HIF1α/TPC2 axis promoted lysosomal Ca^{2+} release and inhibited autophagosome-lysosome fusion in hypoxic PASMCs. PASMCs were divided to control, si-NC, and si-TPC2 groups and treated with hypoxia. (n = 3) (**A**) TEM examination of autophagy. Scale bar, 1 μm. (**B**) Measurement of lysosomal Ca^{2+}. (**C**) Autophagic flux was analyzed through mRFP-GFP-LC3 transfection. Red indicates mRFP, and Green indicates GFP. Scale bar, 20 μm. (**D**) LC3 and p62 were analyzed via western blot. (**E**) Cell migration was assessed by transwell assays. $^{*}P < 0.05$, $^{**}P < 0.01$ and $^{***}P < 0.001$. Original blots/gels are presented in Supplementary Fig. 4–8.

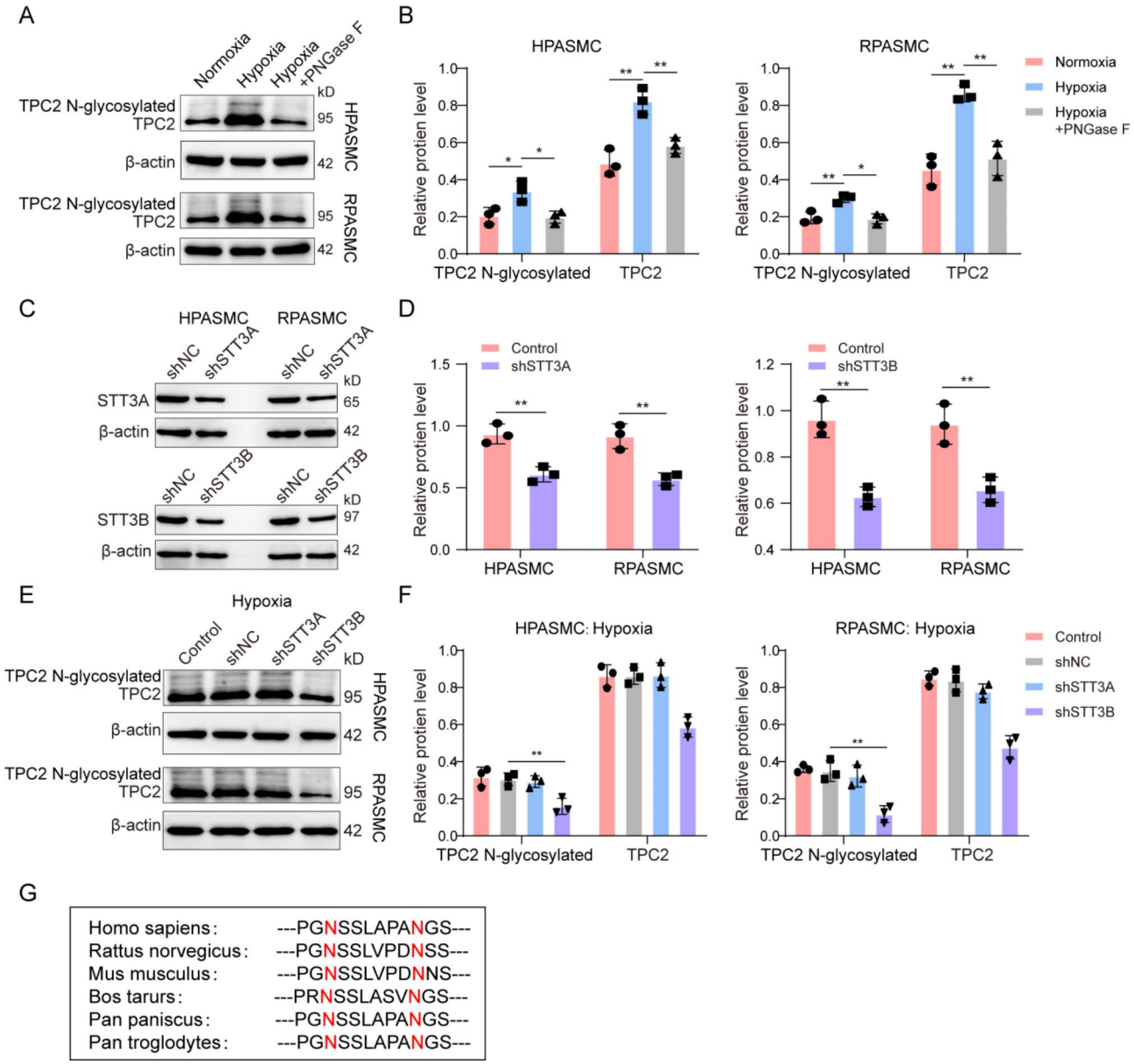

Fig. 5. Hypoxia induced STT3B-mediated TPC2 glycosylation. (**A** and **B**) TPC2 glycosylation in PASMCs treated with normaxia, hypoxia or hypoxia + PNGase F was determined by western blot. (**C** and **D**) The expression of STT3A and STT3B in STT3A or STT3B-silencing PASMCs was analyzed by western blot. (**E** and **F**) TPC2 glycosylation in STT3A or STT3B-silencing PASMCs was determined by western blot. (**G**) The putative glycosylation site of TPC2 was highly conserved in human, nonhuman primates and other mammals and shown in red. $^{*}P < 0.05$, $^{**}P < 0.01$ and $^{***}P < 0.001$. Original blots/gels are presented in Supplementary Fig. 4–8.

and glycosylation of TPC2 we identified, can repress autophagy during the progression of PAH. The regulation of autophagy during PAH needs further investigations.

HIF1α is a heterodimeric transcription factor that functions as a master regulator of cellular adaption to hypoxia and play key roles in various diseases[42,43]. Increased HIF1α expression was observed in lung tissue from PAH patients[44,45], and the cross-regulation of CD146 and HIF1α promoted a synthetic phenotype in PASMCs and targeting the CD146-HIF1α axis improved experimental PAH[46]. Iwona Fijalkowska et al. observed that HIF1α modulated the metabolic shift in PAH[47]. However, the activity of dysregulated HIF1α and its downstream signaling in PAH have not been well addressed. In addition, the link of HIF1α to TPC2 in PAH has never been reported. In the present study, we firstly demonstrated that HIF1α transcriptionally activated TPC2 expression in PAH. More importantly, for the first time, we reported that STT3B initiated the glycosylation of TPC2 in PAH. Further functional analysis showed that hypoxia induced TPC2 expression and subsequent STT3B-dependent TPC2 glycosylation suppressed autophagic flux and PASMC migration, identifying a novel regulatory mechanism responsible for the upregulation and glycosylation of TPC2 and suppression of autophagy in PAH.

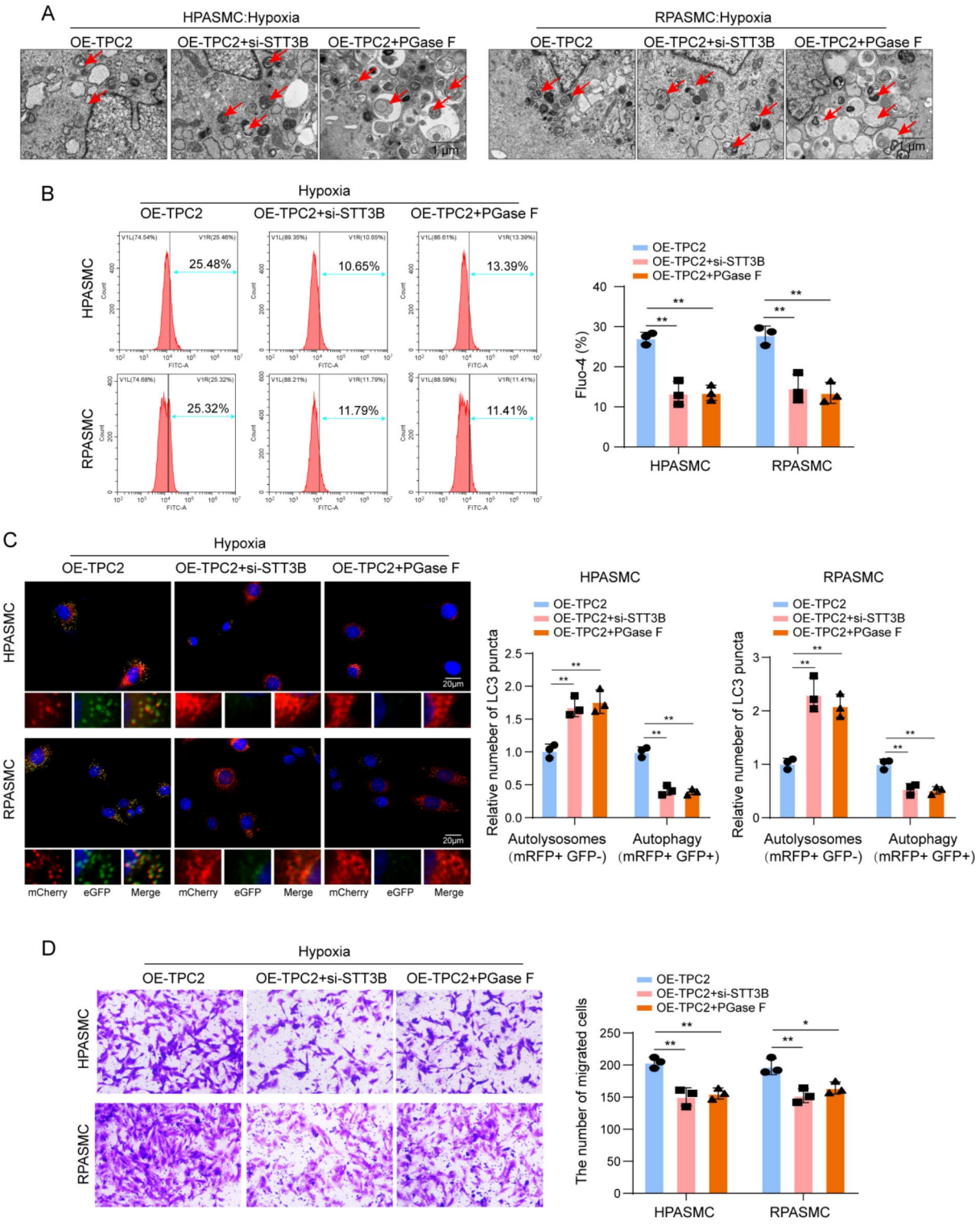

Fig. 6. STT3B-dependent TPC2 glycosylation inhibited autophagic flux and enhanced migration in hypoxic PASMCs. Human and rat PASMCs were divided into OE-TPC2, OE-TPC2 + si-STT3B and OE-TPC2 + PNGaseF groups and treated with hypoxia. (n = 3) (**A**) TEM examination of autophagy. Scale bar, 1 μm. (**B**) Measurement of lysosomal Ca^{2+}. (**C**) Autophagic flux was analyzed through mRFP-GFP-LC3 transfection. Red indicates mRFP, and Green indicates GFP. Scale bar, 20 μm. (**D**) Cell migration was assessed by transwell assays. $^{*}P < 0.05$, $^{**}P < 0.01$ and $^{***}P < 0.001$.

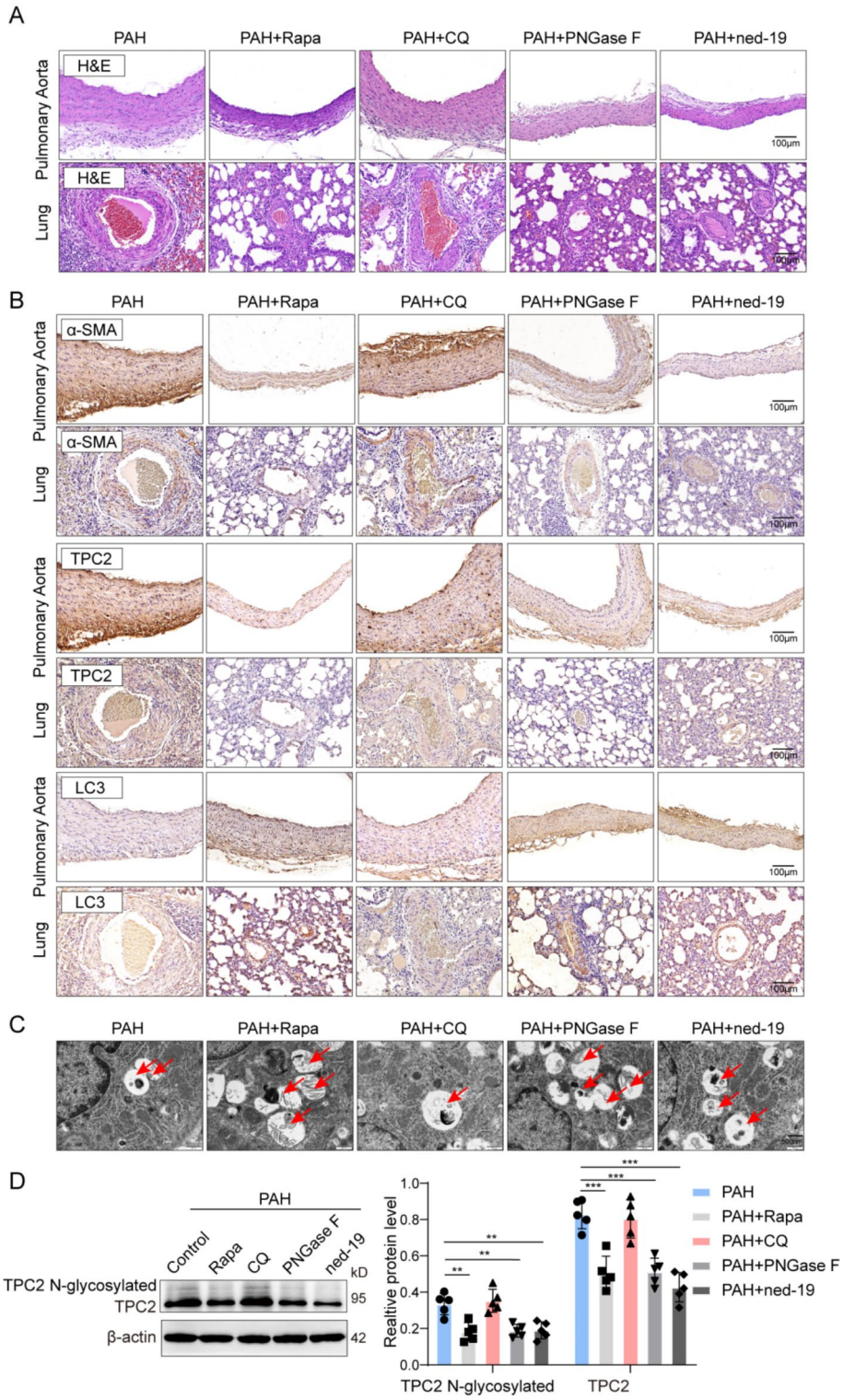

Fig. 7. Inhibition of TPC2 promoted autophagy and alleviated PAH in rats. Rats were divided into PAH, PAH + Rapamycin, PAH + Chloroquine, PAH + PNGase F and PAH + Ned-19 groups. (n = 5) (**A**) H&E staining of pulmonary aorta and the lung. Scale bar, 100 μm. (**B**) IHC staining of α-SMA, TPC2 and LC3. Scale bar, 100 μm (**C**) TEM examination of autophagy in the lung tissue. Scale bar, 500 nm. (**D**) Western blot analysis of TPC2 and its glycosylation. *P < 0.05, **P < 0.01 and ***P < 0.001. Original blots/gels are presented in Supplementary Fig. 4–8.

Group	RV/(LV + S)	HCT (%)	mPAP (mmHg)	mAP (mmHg)	HR
Control (n = 5)	0.21 ± 0.01	35.1 ± 1.02	26.6 ± 0.93	90.2 ± 4.3	393.2 ± 3.9
PAH (n = 5)	0.51 ± 0.02	60.8 ± 1.64	40.8 ± 1.15	99.5 ± 5.8	385.1 ± 3.2

Table 3. Data analysis of different processing groups.

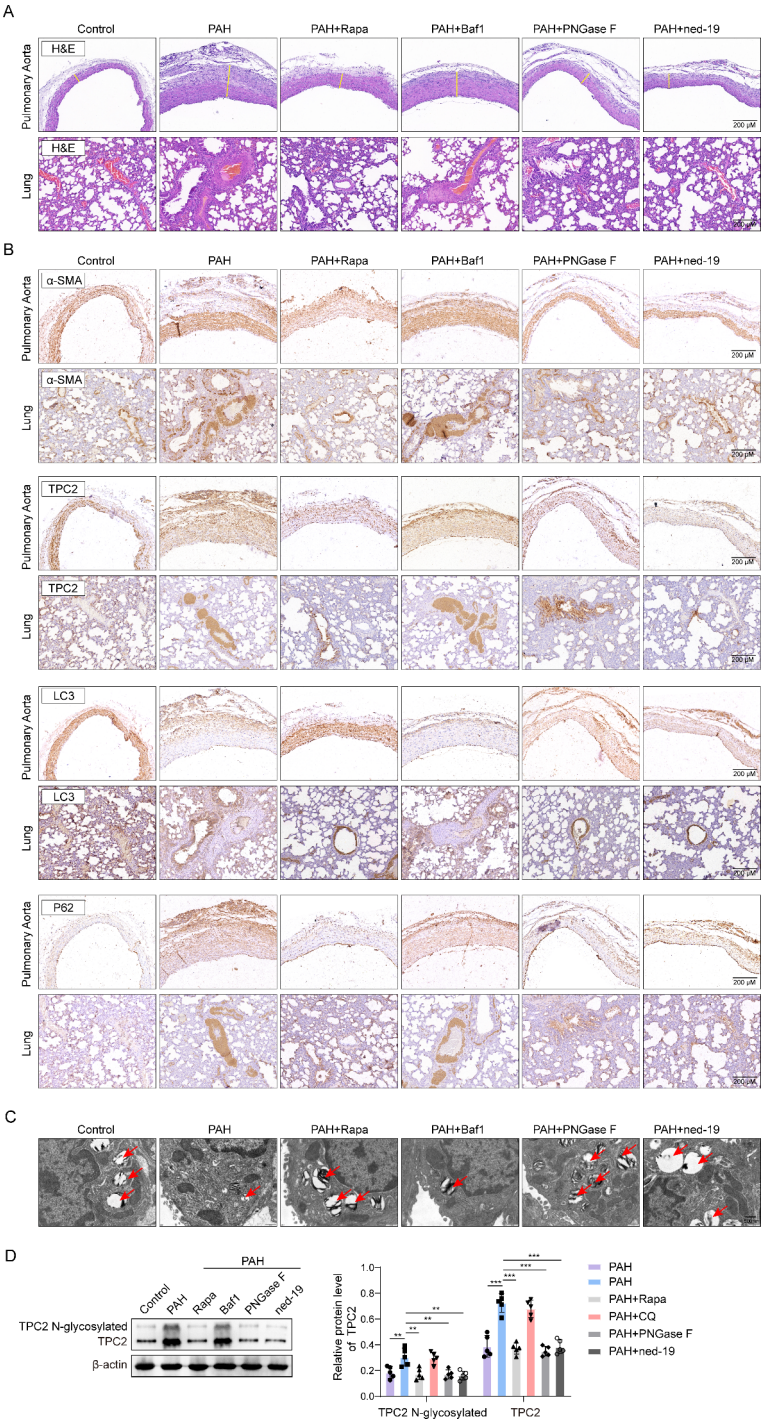

Fig. 8. Baf A1 administration showed no significant effects on PAH rats. SD rats were divided into Control, PAH, PAH + rapa, PAH + Baf A1, PAH + GNGnase and PAH + ned19 groups (n = 5). (**A**) H&E staining of pulmonary aorta and the lung. (**B**) The expression of α-SMA, LC3 and p62 was detected via IHC staining. (**C**) TEM examination of autophagy. Scale bar, 500 nm. (**D**) Western blot analysis of TPC2 and its glycosylation. *P < 0.05, **P < 0.01 and ***P < 0.001. Original blots/gels are presented in Supplementary Fig. 4–8.

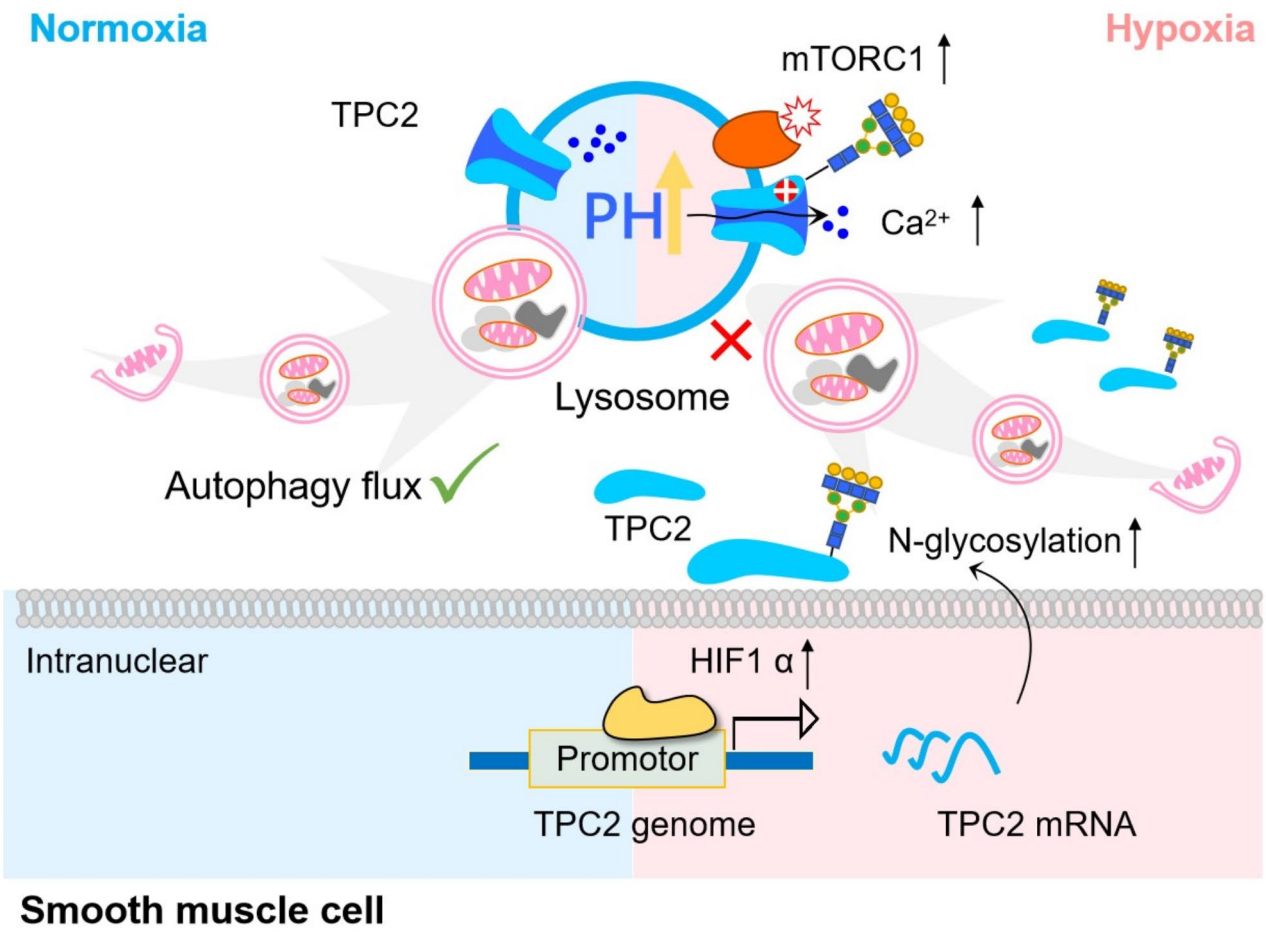

Fig. 9. The mechanical diagram of this study. HIF1α activates TPC2 expression, and increased STT3B-dependent TPC2 glycosylation promotes PASMC proliferation in response to hypoxia and exacerbates PAH via blocking autophagy.

The involvement of HIF1α in STT3B-dependent TPC2 glycosylation remains unclear. A possible mechanism is that hypoxia promotes the expression of glycosyltransferases such as STT3B in a HIF1α-dependent manner[48,49]. Besides, the mechanisms by which STT3B initiates TPC2 glycosylation and how it is regulated in PAH still need further investigation.

Collectively, we firstly revealed that hypoxia induced HIF1α-dependent expression of TPC2 and STT3B-dependent glycosylation of TPC2 to block autophagic flux via promoting lysosomal Ca^{2+} release, thus aggravating PAH. Our findings identify a novel mechanism underlying the progression of PAH and suggest targeting autophagy and other potential therapeutic targets for PAH management although more details and clinical samples are needed.

Data availability

All data generated or analysed during this study are included in this published article (and its Supplementary Information files). The datasets used and/or analyzed in this study are available upon request from the corresponding author.

Received: 5 February 2024; Accepted: 6 December 2024
Published online: 28 December 2024

References

1. Farber, H. W. & Loscalzo, J. Pulmonary arterial hypertension. *N. Engl. J. Med.* **351**(16), 1655–1665 (2004).
2. Thenappan, T., Ormiston, M. L., Ryan, J. J. & Archer, S. L. Pulmonary arterial hypertension: Pathogenesis and clinical management. *BMJ* **360**, j5492 (2018).
3. Delcroix, M. & Howard, L. Pulmonary arterial hypertension: The burden of disease and impact on quality of life. *Eur. Respir. Rev.* **24**(138), 621–629 (2015).
4. Ruopp, N. F. & Cockrill, B. A. Diagnosis and treatment of pulmonary arterial hypertension: A review. *JAMA* **327**(14), 1379–1391 (2022).
5. Jin, X. et al. Targeting two-pore channels: Current progress and future challenges. *Trends Pharmacol. Sci.* **41**(8), 582–594 (2020).

6. Pitt, S. J., Reilly-O'Donnell, B. & Sitsapesan, R. Exploring the biophysical evidence that mammalian two-pore channels are NAADP-activated calcium-permeable channels. *J. Physiol.* **594**(15), 4171–4179 (2016).
7. Hu, W., Zhao, F., Chen, L., Ni, J. & Jiang, Y. NAADP-induced intracellular calcium ion is mediated by the TPCs (two-pore channels) in hypoxia-induced pulmonary arterial hypertension. *J. Cell. Mol. Med.* **25**(15), 7485–7499 (2021).
8. Jiang, Y. L. et al. Nicotinic acid adenine dinucleotide phosphate (NAADP) activates global and heterogeneous local Ca2+ signals from NAADP- and ryanodine receptor-gated Ca2+ stores in pulmonary arterial myocytes. *J. Boil. Chem.* **288**(15), 10381–10394 (2013).
9. Jiang, Y. et al. Two-pore channels mediated receptor-operated Ca(2+) entry in pulmonary artery smooth muscle cells in response to hypoxia. *Int. J. Biochem. Cell Biol.* **97**, 28–35 (2018).
10. Sun, W. & Yue, J. TPC2 mediates autophagy progression and extracellular vesicle secretion in cancer cells. *Exp. Cell Res.* **370**(2), 478–489 (2018).
11. Gomez-Puerto, M. C. et al. Autophagy contributes to BMP type 2 receptor degradation and development of pulmonary arterial hypertension. *J. Pathol.* **249**(3), 356–367 (2019).
12. Yang, Z., Zhou, L., Ge, H., Shen, W. & Shan, L. Identification of autophagy-related biomarkers in patients with pulmonary arterial hypertension based on bioinformatics analysis. *Open Med.* **17**(1), 1148–1157 (2022).
13. Schwarz, F. & Aebi, M. Mechanisms and principles of N-linked protein glycosylation. *Curr. Opin. Struct. Boil.* **21**(5), 576–582 (2011).
14. Gong, Q., Anderson, C. L., January, C. T. & Zhou, Z. Role of glycosylation in cell surface expression and stability of HERG potassium channels. *Am. J. Physiol. Heart Circ. Physiol.* **283**(1), H77-84 (2002).
15. Egenberger, B., Polleichtner, G., Wischmeyer, E. & Doring, F. N-linked glycosylation determines cell surface expression of two-pore-domain K+ channel TRESK. *Biochem. Biophys. Res. Commun.* **391**(2), 1262–1267 (2010).
16. Hooper, R., Churamani, D., Brailoiu, E., Taylor, C. W. & Patel, S. Membrane topology of NAADP-sensitive two-pore channels and their regulation by N-linked glycosylation. *J. Boil. Chem.* **286**(11), 9141–9149 (2011).
17. Liu, K. et al. Hypoxia-induced GLT8D1 promotes glioma stem cell maintenance by inhibiting CD133 degradation through N-linked glycosylation. *Cell Death Differ.* **29**(9), 1834–1849 (2022).
18. Schjoldager, K. T., Narimatsu, Y., Joshi, H. J. & Clausen, H. Global view of human protein glycosylation pathways and functions. *Nat. Rev. Mol. Cell. Biol.* **21**(12), 729–749 (2020).
19. Bueno-Beti, C., Sassi, Y., Hajjar, R. J. & Hadri, L. Pulmonary artery hypertension model in rats by monocrotaline administration. *Methods Mol. Boil.* **1816**, 233–241 (2018).
20. Yla-Anttila, P., Vihinen, H., Jokitalo, E. & Eskelinen, E. L. Monitoring autophagy by electron microscopy in Mammalian cells. *Methods Enzymol.* **452**, 143–164 (2009).
21. Feijoo-Bandin, S. et al. Two-pore channels (TPCs): Novel voltage-gated ion channels with pleiotropic functions. *Channels* **11**(1), 20–33 (2017).
22. Garcia-Rua, V. et al. Endolysosomal two-pore channels regulate autophagy in cardiomyocytes. *J. Physiol.* **594**(11), 3061–3077 (2016).
23. Young, J. M., Williams, D. R. & Thompson, A. A. R. Thin air, thick vessels: Historical and current perspectives on hypoxic pulmonary hypertension. *Front. Med.* **6**, 93 (2019).
24. Medina, D. L. et al. Lysosomal calcium signalling regulates autophagy through calcineurin and TFEB. *Nat. Cell Biol.* **17**(3), 288–299 (2015).
25. Li, S. S. et al. Monitoring the changes of pH in lysosomes during autophagy and apoptosis by plasmon enhanced Raman imaging. *Anal. Chem.* **91**(13), 8398–8405 (2019).
26. Semenza, G. L. Hypoxia-inducible factor 1: Master regulator of O2 homeostasis. *Curr. Opin. Genet. Dev.* **8**(5), 588–594 (1998).
27. Cherepanova, N. A., Venev, S. V., Leszyk, J. D., Shaffer, S. A. & Gilmore, R. Quantitative glycoproteomics reveals new classes of STT3A- and STT3B-dependent N-glycosylation sites. *J. Cell Biol.* **218**(8), 2782–2796 (2019).
28. Quan, W., Lim, Y. M. & Lee, M. S. Role of autophagy in diabetes and endoplasmic reticulum stress of pancreatic beta-cells. *Exp. Mol. Med.* **44**(2), 81–88 (2012).
29. Menzies, F. M., Fleming, A. & Rubinsztein, D. C. Compromised autophagy and neurodegenerative diseases. *Nat. Rev. Neurosci.* **16**(6), 345–357 (2015).
30. Mulcahy Levy, J. M. & Thorburn, A. Autophagy in cancer: moving from understanding mechanism to improving therapy responses in patients. *Cell Death Differ.* **27**(3), 843–857 (2020).
31. Lee, S. J. et al. Autophagic protein LC3B confers resistance against hypoxia-induced pulmonary hypertension. *Am. J. Respir Crit. Care Med.* **183**(5), 649–658 (2011).
32. Long, L. et al. Chloroquine prevents progression of experimental pulmonary hypertension via inhibition of autophagy and lysosomal bone morphogenetic protein type II receptor degradation. *Circ. Res.* **112**(8), 1159–1170 (2013).
33. Feng, W. et al. Paclitaxel alleviates monocrotaline-induced pulmonary arterial hypertension via inhibition of FoxO1-mediated autophagy. *Naunyn-Schmiedeberg's Arch. Pharmacol.* **392**(5), 605–613 (2019).
34. Kim, J., Kundu, M., Viollet, B. & Guan, K. L. AMPK and mTOR regulate autophagy through direct phosphorylation of Ulk1. *Nat. Cell Biol.* **13**(2), 132–141 (2011).
35. Goncharova, E. A., Simon, M. A. & Yuan, J. X. mTORC1 in pulmonary arterial hypertension. At the crossroads between vasoconstriction and vascular remodeling?. *Am. J. Respir. Crit. Care Med.* **201**(10), 1177–1179 (2020).
36. Zhang, H. et al. Apelin inhibits the proliferation and migration of rat PASMCs via the activation of PI3K/Akt/mTOR signal and the inhibition of autophagy under hypoxia. *J. Cell. Mol. Med.* **18**(3), 542–553 (2014).
37. Han, X. et al. Impaired V-ATPase leads to increased lysosomal pH, results in disrupted lysosomal degradation and autophagic flux blockage, contributes to fluoride-induced developmental neurotoxicity. *Ecotoxicol. Environ. Saf.* **236**, 113500 (2022).
38. Kawai, A., Uchiyama, H., Takano, S., Nakamura, N. & Ohkuma, S. Autophagosome-lysosome fusion depends on the pH in acidic compartments in CHO cells. *Autophagy* **3**(2), 154–157 (2007).
39. Yuan, Y. et al. Segregated cation flux by TPC2 biases Ca(2+) signaling through lysosomes. *Nat. Commun.* **13**(1), 4481 (2022).
40. Zhang, X. et al. Puerarin prevents progression of experimental hypoxia-induced pulmonary hypertension via inhibition of autophagy. *J. Pharmacol. Sci.* **141**(2), 97–105 (2019).
41. Yamanaka, R. et al. TIGAR reduces smooth muscle cell autophagy to prevent pulmonary hypertension. *Am. J. Physiol. Heart Circ. Physiol.* **319**(5), H1087–H1096 (2020).
42. Masoud, G. N. & Li, W. HIF-1alpha pathway: Role, regulation and intervention for cancer therapy. *Acta Pharmaceut. Sin. B* **5**(5), 378–389 (2015).
43. Weidemann, A. & Johnson, R. S. Biology of HIF-1alpha. *Cell Death Differ.* **15**(4), 621–627 (2008).
44. Bonnet, S. et al. An abnormal mitochondrial-hypoxia inducible factor-1alpha-Kv channel pathway disrupts oxygen sensing and triggers pulmonary arterial hypertension in fawn hooded rats: Similarities to human pulmonary arterial hypertension. *Circulation* **113**(22), 2630–2641 (2006).
45. Lei, W. et al. Expression and analyses of the HIF-1 pathway in the lungs of humans with pulmonary arterial hypertension. *Mol. Med. Rep.* **14**(5), 4383–4390 (2016).
46. Luo, Y. et al. CD146-HIF-1alpha hypoxic reprogramming drives vascular remodeling and pulmonary arterial hypertension. *Nat. Commun.* **10**(1), 3551 (2019).

47. Fijalkowska, I. et al. Hypoxia inducible-factor1alpha regulates the metabolic shift of pulmonary hypertensive endothelial cells. *Am. J. Pathol.* **176**(3), 1130–1138 (2010).
48. Silva-Filho, A. F. et al. Glycobiology modifications in intratumoral hypoxia: The breathless side of glycans interaction. *Cell. Physiol. Biochem.* **41**(5), 1801–1829 (2017).
49. Arriagada, C., Silva, P. & Torres, V. A. Role of glycosylation in hypoxia-driven cell migration and invasion. *Cell Adhes. Migrat.* **13**(1), 13–22 (2019).

Acknowledgements
The authors acknowledge the work of all investigators involved in the present study.

Author contributions
Chao Li and YongLiang Jiang conceived the original idea for the study.Chao Li, Cheng Li and YongLiang Jiang participated in the design and supervision of the study. Chao Li wrote the first draft of the manuscript and the final content was developed in collaboration with all authors. YuFei Jiang, MoFei Liu, ChengYi Yang, JiaXin Lu: contributed to acquisition of data. YongLiang Jiang: contributed to conception, design of study, and revision of the manuscript. All authors saw and approved the final version of the manuscript.

Funding
This work was supported by the grant from by the National Natural Science Foundation of China (82400050,82070057), and the Natural Science Foundation of Hunan (2021JJ30400,2024JJ6270), and the Natural Science Foundation of Changsha (kq2014191), and the Young Doctor Foundation of Hunan Provincial People's Hospital (BSJJ202215).

Declarations

Ethics approval and consent to participate
All animal experiments were conducted in accordance with the Guide for the Care and Use of Laboratory Animals which was approved by the Institutional Animal Care Committee (IACUC) and the Experimental Animal Committee of Hunan Normal University (No.2022103218). This study follows the ARRIVE guidelines. We followed all relevant ethical standards during the study and ensured the welfare of all laboratory animals.

Competing interests
The authors declare no competing interests.

Additional information
Supplementary Information The online version contains supplementary material available at https://doi.org/10.1038/s41598-024-82552-y.

Correspondence and requests for materials should be addressed to Y.J.

Reprints and permissions information is available at www.nature.com/reprints.

Publisher's note Springer Nature remains neutral with regard to jurisdictional claims in published maps and institutional affiliations.